First-principle Band Structure Calculations of Tris(8-hydroxyquinolinato)aluminum

Yanting Yang,[†,‡] Hua Geng,[‡] Shiwei Yin,[‡] Zhigang Shuai,*[,‡] and Junbiao Peng*[,†]

Institute of Polymer Optoelectronic Materials and Devices, Key Laboratory of Specially Functional Materials and Advanced Manufacturing Technology, South China University of Technology, 510640 Guangzhou, China, Key Laboratory of Organic Solids, Institute of Chemistry, Chinese Academy of Sciences, 100080 Beijing, China

Received: July 21, 2005; In Final Form: December 7, 2005

Tris(8-hydroxyquinolinato)aluminum (Alq_3) has been widely used in organic light-emitting diodes (OLEDs) both as electron transport and light-emitting materials. To gain a deeper understanding for its carrier transport properties, we carry out first-principle band-structure calculations using density-functional theory with generalized gradient approximation by the Becke exchange plus Lee−Yang−Parr correlation functional. The intermolecular interaction related to transport behavior has been analyzed from the Γ-point wave function as well as from the bandwidths and band gaps. From the calculated bandwidths of the frontier bands as well as the effective masses of the electron and the hole, we conclude that the mobility of electron is about 2−3 times larger than that for the hole. Furthermore, when several bands near Fermi surface are taken into account, we find that the interband gaps within the unoccupied bands are generally smaller than those for the occupied bands, which indicate that the electron can hop from one band to another, much easier than the hole, through electron−phonon coupling for instance, thus, effectively representing an even larger mobility for the electron than for the hole. Therefore, from both the intra-band and inter-band processes point of view, the theory shows that that Alq_3 is a good electron transport material.

I. Introduction

The organic light-emitting diodes (OLEDs) have played an important role both in display and in solid-state lighting technology, which attracts intense investigation, both academia and industrial.[1] The emitting materials range from conjugated polymers[2,3] to small molecules[4] and to organo-metalics.[5] Tris(8-hydroxyquinolate)aluminum (Alq_3) is the first and the most important electroluminescent material currently used in OLEDs.[6] Great efforts have been made to improve the efficiency and stability of the OLEDs devices, as well as the emission colors.[7−9]

There have been many fundamental studies on metaloquinolates in recent years in revealing the structural and electronic properties of Alq_3,[10−23] many of which have been carried out on ground-state characteristics. Alq_3 has two geometric isomers: the facial (*fac*-Alq_3) and the meridianal (*mer*-Alq_3) forms, having C_3 and C_1 symmetries, respectively. The *mer*-Alq_3 form was found to be energetically more stable than the facial structure. The *fac*-Alq_3 structure can be reconverted to the meridianal form during evaporation onto unheated substrates or after dissolving it in polar solvents.[24] The vertical electronic excitation energies of Alq_3 have been computed with molecular orbital methods.[7,17−20] In these theoretical studies, both the configuration interaction (CI) approach with the semiempirical ZINDO Hamiltonian[21] and the first-principle time-dependent density functional theory (TD−DFT) have been used to compute the vertical excitation spectra[7,17−19] and the electro-absorption[20] of Alq_3. Recently, the lowest singlet excited state (S_1) of Alq_3 has been optimized by the ab initio singles configuration interaction (CIS) method.[22,23] The emission properties are calculated based on the excited-state structure by either semiemipirical ZINDO, ab initio CIS, or first-principle TD−DFT.[22,23] The energy partitioning analysis of the bonding between the metal fragment $Alq2^+$ and a single ligand q^- in Alq3 in its ground (S_0) state has also been performed.[25]

We note that generally, the organic molecules are good hole transport materials. From band structure point of view, the occupied bands in organic solids usually present larger bandwidths than the unoccupied bands. However, Alq_3 is an excellent electron transport material, in addition to being excellent light-emitting material.[6]

In this work, we are most interested in the transport-related electronic structures of Alq_3. In fact, the study of charge-carrier mobilities in organic molecular crystals has been a hotly debated subject for the past decades,[26,27] and it still stays as an unresolved issue.[28,29] The carrier mobility is one of the most important factor for organic electronics applications. In the well ordered organic crystals, the transport at low temperature is governed by a coherent band-like picture, where the mobility can attain a few tens of cm^2/Vs,[30,31] and follows the power law on temperature (T^{-n}). At room temperature, carriers move with lattice deformation through thermally activated hopping process, which can be described by an Arrhenius law on temperature.[32,33] Recently, Lin et al. have described the hopping process by Marcus electron transfer theory and used Hartree−Fock Koopmans' theorem coupled with a direct coupling scheme to calculate the charge-transfer (hopping) integral based on a molecular dimer model, regarding different relative positions for two molecules of *mer*-Alq_3 in an amorphous film.[34] They found that the coupling factor for electrons is more than an order of magnitude larger than the hole in all the directions, indicating that the electron mobility is more than 2 orders of magnitude larger than the hole.

* Corresponding authors' e-mail: zgshuai@iccas.ac.cn, psjbpeng@scut.edu.cn.
† South China University of Technology.
‡ Chinese Academy of Sciences.

10.1021/jp0540252 CCC: $33.50
Published on Web 01/31/2006

We believe that long-range molecular interaction plays an important role in determining the transport properties. Even though the material structure in the device is amorphous, knowledge based on a well ordered crystal structure presents a reference standard for understanding the electronic properties without disorders, which will facilitate to reveal the intrinsic behaviors of the materials. The effect of disorder can be considered separately. Therefore, an investigation taking the crystal symmetry into account is essential to interpret and to better understand the transport mechanism of the Alq_3 crystal. We note that in the literature, the first-principle band structure calculations on organic crystals have been vastly ignored, probably due to the fact that in organic crystals, the intermolecular interaction is dominated by a weak van der Waals force, and the intermolecular distance is large; the electron density variation is much more pronounced than in inorganic crystals. Nevertheless, to a large extent, this problem can be remedied by taking the density gradient into the functional in the generalized gradient approximation (GGA) in density functional theory (DFT).

In this paper, we calculated the band structure of the Alq_3 crystal. To the best of our knowledge, this work represents the first one based on the first-principle method. The bottom line is that the band picture transport mechanism dominates in a low-temperature regime. We will first analyze the frontier bands (near Fermi surface) structure in terms of bandwidths and band gaps. Then we will make an analysis on the wave functions in the Γ-point in order to realize molecular interaction and splitting of the frontier molecular orbitals. The transport properties for electrons and for holes are obtained through the effective masses under the constant relaxation time approximation.

II. Theoretical Background and Methodology

For the hopping regime (at room temperature), the transport related electronic structure calculations on organic solids have been extensively studied through the electronic level splittings evaluation[35] within the Koopmans' theorem using the semiempirical intermediate neglect of differential overlap (INDO) method. Cornil and co-workers have first looked at the prototypical conjugated polyene, trans-stilbene, pentacene, etc in a cofacial dimer configuration. Interestingly, the INDO method typically provides transfer integrals comparable to those obtained with DFT-based approaches.[36,37] Such quantum-chemistry based calculations have been indeed used to help molecular design, prior to synthesis, for new discotic mesogens, whose transport properties are shown to be less affected by intermolecular orientation. This is the case, for instance, for hecaazatriisothianaphthenes[38] and triphenylene derivatives incorporating nitrogen atoms in the exterior rings.[39]

For band picture description, for instance, in the case of the oligoacene single crystals, the evaluation of three-dimensional band-structures based on the INDO-calculated splittings between adjacent molecules, leads to very significant bandwidths both for the valence and conduction bands.[40] Bobbert and co-workers have started from band-structure of oligoacene crystal and the electron−phonon interaction (including its induced bandwidth narrowing effects) and gave a qualitatively correct temperature dependence of the carrier mobilities.[41] Very recently, Troisi and Orlandi have developed a molecular frontier orbital-based tight-binding model to calculate the frontier orbital band structures of pentacene in four different polymorphs,[42] where all the coupling constants (parameters for tight-binding model) is evaluated through a direct first-principle method, instead of

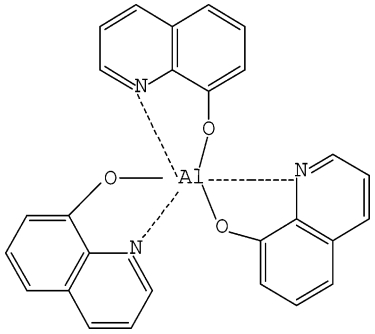

Figure 1. Molecular structure of tris(8-hydroxyquinoline) aluminum (Alq_3).

Koopmans' theorem. Within the band picture, the velocity of carrier is obtained as

$$\vec{v}(k) = \nabla_k E(k)/\hbar \tag{1}$$

where $E(k)$ is the band structure of organic crystal. Under the constant relaxation time approximation at low temperature, and by assuming that only the carriers near Fermi surface contribute to the transport, the mobility can be simply obtained as

$$\mu_\alpha\beta = e\tau(m^{-1})_\alpha\beta \tag{2}$$

where τ is the temperature-dependent averaged relaxation time, and

$$(m^{-1})_\alpha\beta = -\frac{1}{\hbar^2}\left(\frac{\partial^2 E(k)}{\partial k_\alpha \partial k_\beta}\right) \tag{3}$$

is the inverse of effective mass. The α and β are the cartesian indices. Namely, the heavier the effective mass, the smaller the mobility. Thus, under such approximation, band structure knowledge is enough to reveal the transport behavior.

There exist four solvent-free crystals structures for Alq_3:[43−46] α-, β-phase, and high-temperature (>380 °C) δ- and γ-phase. The UV−vis and fluorescence spectra in the amorphous film closely resemble those of the β-phase.[44] Therefore, the crystal structure in this work is chosen to be β-phase, which belongs to the space group $P\bar{1}$, and in each unit cell there are two molecules related by inversion symmetry. We know that if there are two inequivalent molecules (say, type A and type B) in one cell, there will be two bands arising from the symmetric and antisymmetric combinations of molecular wave functions in a cell, both for electron and for hole bands.[40] Assuming the concentration of charge carriers is very small, a one-particle formalism is applicable, and the excess electron or hole does not significantly change the wave function of the molecule, then the lowest unoccupied molecular orbital (LUMO) of a molecule can be used as a basis for crystal electron wave functions, and the highest occupied orbital (HOMO) can be used for hole wave functions.[40]

We use density-functional theory, DFT−GGA with Becke exchange plus Lee−Yang−Parr correlation (BLYP) functional, as implemented in Dmol[3] within the Materials Studio package[47,48] to calculate the band structure of the crystalline Alq_3 along high-symmetry directions in the first Brillouin zone, as well as the Γ point wave function. Here we focus on the meridianal isomer with optimized molecular geometry (see Figure 1). The lattice parameters we used are a = 8.443 Å, b = 10.252 Å, c = 13.171 Å, α = 108.58°, β = 97.06°,

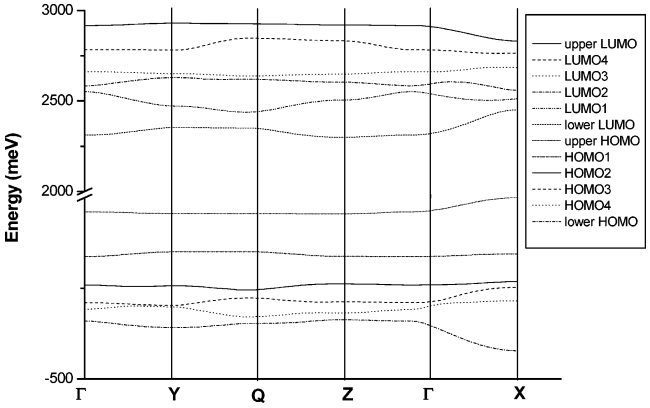

Figure 2. Band structure of Alq_3.

$\gamma = 89.74°$.[45] Integrations over the Brillouin zone were carried out by using the Monkhorst−Pack scheme[49] with $10 \times 10 \times 10$ k-sampling in the relevant irreducible wedge.

III. Results and Discussion

The calculated band structure is depicted in Figure 2. The k-space symmetry points are chosen to be: Γ (0, 0, 0), Y (0, 1/2, 0), Q (0, 1/2, 1/2), Z (0, 0, 1/2), and X (1/2, 0, 0). The dispersion curves are displayed along direction Γ→Y→Q→Z→Γ→X with 20 k-points in each segment. To reveal the molecular orbital contributions to the crystal orbital and to disclose the molecular origin of the energy band, we first make an analysis on the wave functions at the Γ-point ($k = 0$), which is plotted in one unit cell, with yellow (blue) color for positive (negative) wave function values, respectively, see Figure 3. As there are two molecules in unit cell, supramolecular orbital can be regarded as a linear combination of the two molecules:

$$\Psi_{uc1}(r) = \frac{1}{\sqrt{2}}(\Psi_k^{\,1} - \Psi_k^{\,2})$$

$$\Psi_{uc2}(r) = \frac{1}{\sqrt{2}}(\Psi_k^{\,1} + \Psi_k^{\,2}) \qquad (4)$$

Here Ψ_k^1 and Ψ_k^2 are the specific molecular orbitals for molecule 1 and 2, respectively, and $\Psi_{uc}(r)$is the unit-cell orbital. Take the molecular LUMO as an example. The intermolecular interaction results in a splitting for the LUMO, represented by the two ψ_{uc}'s. From the Γ-point orbital, we can analyze the relative signs of two molecules, from which we can realize which two supramolecular orbitals correspond to a specific mono-molecular orbital splitting. Therefore, we can refer a particular band to a molecular orbital. Figure 3(a) is the wave function for the lowest unoccupied band. From the Γ-point wave functions plot, we can clearly see that it is the fifth band above it that corresponds to its counterpart according to eq 4. Namely, these two bands correspond to the molecular LUMO. Similar situation is found for the molecular HOMO bands. It is interesting to note that these two bands do not merge to form one band. This is due to the triclinic crystal symmetry of Alq_3. Previous theoretical investigations have often used total bandwidths as criteria for comparing intrinsic excess electron and excess hole mobilities. It is not appropriate for triclinic crystal structure. Due to the triclinic structure, the degeneracy at the Brillouin zone edge is removed, thus there a gap appears between the two components of the molecular orbital splitting.[37] This implies that the molecular orbital splitting is not necessarily equivalent to bandwidth for crystal. In such a case, only a full band structure calculation can reveal the actual bandwidth, as well as band gap. In Table 1, we present the bandwidths and inter-band gaps for the upper and lower HOMO and LUMO bands.

Looking at Table 1, we find that the HOMO splitting (with the largest value of 614.44 meV in the Z→G direction) is, in general, larger than the LUMO splitting (with the largest value of 531.68 meV). This could easily lead to the conclusion that the hole mobility is larger than the electron. However, if we compare the bandwidths of the lower LUMO and the upper HOMO bands, which are more pertinent to the carrier transport, the former is more than 3 times larger than the latter. This is in good agreement with the experimental results that Alq_3 is an excellent electron transport material.

If we take a look at the band structures near Fermi level for bands other than the HOMO and LUMO, we can see that (i) the bandwidths are, in general, much larger than those of the occupied bands, and (ii) the band gaps between the unoccupied bands are, in general, smaller than those between the occupied bands, see Table 2. The former further confirms our previous analysis based on HOMO and LUMO bands. The latter fact implies that if we take the interband transition due to scattering effects from thermal motion, the electron would move even more easily than the hole.

We further calculated the effective masses of electron and hole from the band structure data. We first locate the minima of the HOMO and the LUMO bands. Then we performed numerical second-order derivatives of *E(k)* with respect to *k* according to eq 3.

The inverse electron effective mass matrix is obtained to be

$$m_{el}^{-1} = \begin{pmatrix} 0.4878 & -0.0029 & 0.015 \\ -0.0029 & 0.1743 & -0.0044 \\ 0.015 & -0.0044 & 0.0388 \end{pmatrix} \qquad (5)$$

A direct diagonalization of the above matrix gives the following eigen values: 0.4883, 0.1756, and 0.036953. It is seen that the nondiagonal parts do not play any appreciable role, because the eigen values are close to the diagonal parts of eq 5, namely the principal axis of transport almost coincides with the original unit cell vectors. For hole, we have

$$-m_h^{-1} = \begin{pmatrix} 0.2236 & -0.1008 & 0.0038 \\ -0.1008 & 0.0957 & 0.0218 \\ 0.0038 & 0.0218 & 0.0333 \end{pmatrix} \qquad (6)$$

The eigen values are 0.2787, 0.0582, and 0.0157. The effective masses are obtained to be a few times of bare electron mass. It should be noted that, for inorganic semiconductors, the effective mass is usually less than one tenth of a bare electron mass m_e. For instance, in GaAs, the electron and hole effective masses are $0.067m_e$ and $0.08m_e$, respectively. Roughly speaking, the effective mass for the hole is 2−3 times as large as that for the electron. From a band picture point of view, the inverse of effective mass is proportional to the mobility. Then, it indicates the electron mobility should be 2−3 times larger than that for the hole, if we assume the same relaxation time constants.

Thus, both from the intraband and interband motion, the first principle band structure calculations do demonstrate that Alq_3 is indeed a good electron transport material, in qualitative agreement with the results based on hopping mechanism calculations by Lin et al.[34] It is understood that in their approach,

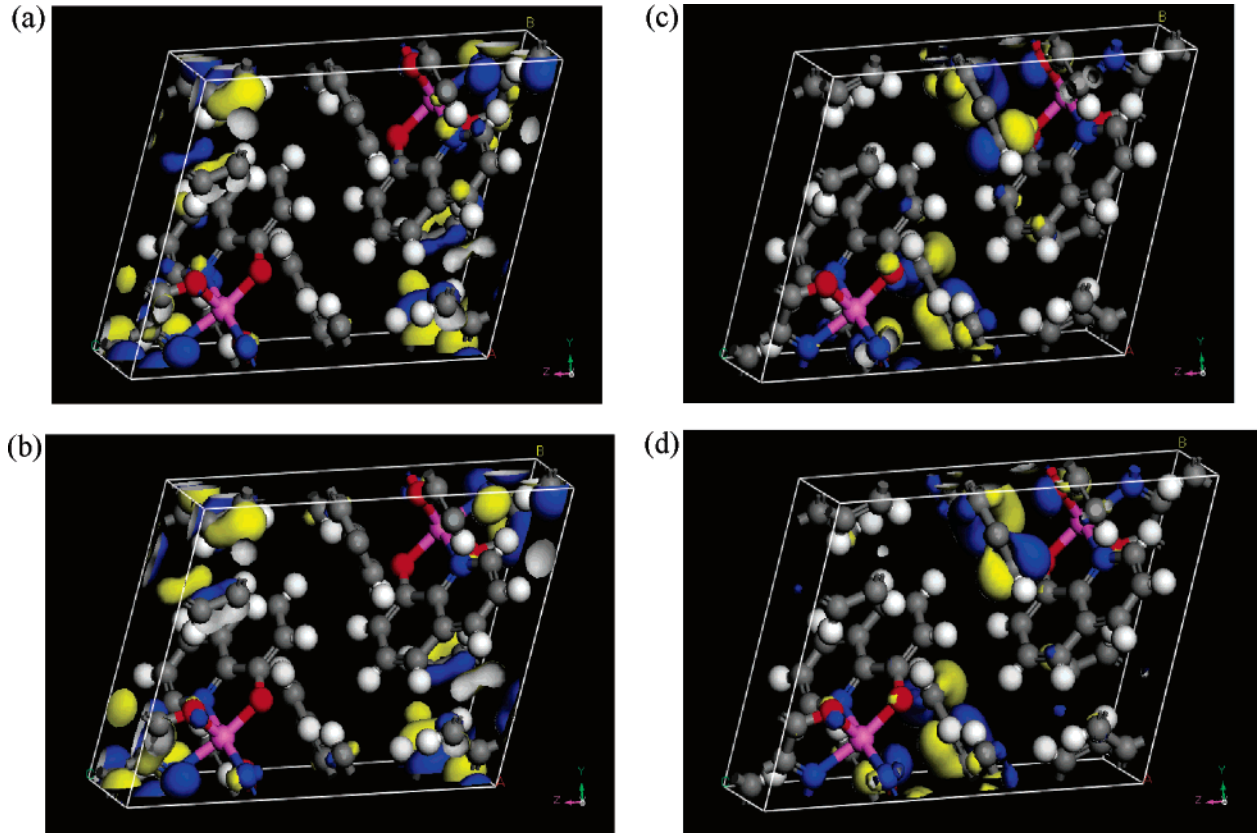

Figure 3. Γ- point wave function plots for (a) LUMO orbital; (b) The fifths upper LUMO orbital; (c) The HOMO orbital; and (d) The fifths lower HOMO orbital at the Γ point.

TABLE 1: Band Structure Data for the Upper and Lower of HOMO and LUMO Bands (in meV)

		Γ→Y	Y→Q	Q→Z	Z→G	Γ→X
LUMO	upper LUMO bandwidth	12.52	3.65	4.06	4.32	91.56
	lower LUMO bandwidth	41.36	3.27	41.36	12.52	139.05
	band gap between upper and lower LUMO band	301.13	303.46	292.01	292.01	301.07
	maximum separation between upper and lower LUMO bands	355.01	310.38	337.43	308.85	531.68
HOMO	upper HOMO bandwidth	11.74	0.16	0.98	5.5	38.38
	lower HOMO bandwidth	17.88	11.05	10.34	3.73	81.82
	band gap between upper and lower HOMO bands	576.29	575.39	575.39	605.21	380.72
	maximum separation between upper and lower HOMO bands	605.91	586.6	586.71	614.44	500.92

TABLE 2: Band Structure Data near Fermi Level (in meV)

		Γ→Y	Y→Q	Q→Z	Z→G	Γ→X
unoccupied bands	bandwidth of LUMO+2	48.21	4.76	23.81	10.12	23.81
	gap between LUMO+1 and LUMO+2	23.81	158.93	101.79	28.57	43.45
	bandwidth of LUMO+1	76.79	29.17	57.74	53.57	29.17
	gap between lower LUMO and LUMO+1 bands	116.07	91.67	91.67	222.02	57.75
occupied bands	gap between upper HOMO and HOMO-1	106.19	106.19	106.19	118.08	122.84
	bandwidth of HOMO-1	11.90	0.00	11.90	0.00	7.14
	gap between HOMO-1 and HOMO-2	79.71	93.99	74.96	74.96	74.96
	bandwidth of HOMO-2	2.38	9.52	16.66	4.76	9.82

the interband effects are mixed with the intraband contributions, because for a dimer, there does not exist band structure.

IV. Conclusion

To summarize, we have carried out the first principle calculation on the band structure for Alq_3, an excellent organic electron transport, as well as light emitting material. We focus on discussing its transport related electronic structure. By analyzing the wave function at the Γ point, we are able to identify the electronically active bands with their molecular orbital origin so that we reveal the intermolecular coupling and splitting information. It is found that (i) due to the triclinic crystal

symmetry, both the mono-molecule HOMO and LUMO bands will split into two bands, and the lower LUMO bandwidth is more than three times as large as that for the upper HOMO band; (ii) in general, the unoccupied frontier bands have broader bandwidths and narrower band gaps than those for the occupied frontier bands; (iii) the inverse effective mass of electron is 2−3 times larger than that for the hole. These facts indicate that, in Alq_3, the electrons are the dominant carriers in transport.

Acknowledgment. We are grateful to Prof. Jinlong Yang for discussions on the band-structure calculations and to Dr. David Beljonne for conversations on the transport phenomena in organic crystals. This work is supported by the Ministry of Science and Technology of China through the 973 program (grant 2002CB613400) and National Science Foundation of China (grants 90203015, 90301001, 20420150034, and 10425420). The numerical calculations have been carried out in the CNIC supercomputer center of the Chinese Academy of Sciences.

References and Notes

(1) Miyata, S.; Nalwa, S. *Organic Electroluminescent Materials and Devices*; Gordon and Breach: Amsterdam, The Netherlands, 1997.

(2) Burroughes, J. H.; Bradley, D. D. C.; Brown, A. R.; Marks, R. N.; Mackay, K.; Friend, R. H.; Burns, P. L.; Holmes, A. B. *Nature* **1990**, *347*, 539.

(3) Friend, R. H.; Gymer, R. W.; Holmes, A. B.; Burroughes, J. H.; Marks, R. N.; Taliani, C.; Bradley, D. D. C.; Dos Santos, D. A.; Brédas, J. L.; Logdiund, M.; Salaneck, W. R. *Nature* **1999**, *397*, 121.

(4) Mitsche, U.; Baeuerle, P. *J. Mater. Chem.* **2000**, *10*, 1471.

(5) Baldo, M. A.; O'Brien, D. F.; You, Y.; Shoustikov, A.; Sibley, S.; Thompson, M. E.; Forrest, S. R.; *Nature* **1998**, *395*, 151; O'Brien, D. F.; Baldo, M. A.; Thompson, M. E.; Forrest, S. R. *Appl. Phys. Lett.* **1999**, *75*, 4.

(6) Tang, C. W.; Van Slyke, S. A. *Appl. Phys. Lett.* **1987**, *51*, 913.

(7) Burrows, P. E.; Shen, Z.; Bulovic, V.; McCarty, D. M.; Forrest, S. R.; Cronin, J. A.; Thompson, M. E. *J. Appl. Phys.* **1996**, *79*, 7991.

(8) Hamada, Y. *IEEE Trans. Electron Devices* **1997**, *44*, 1208.

(9) VanSlyke, S. A.; Chen, C. H.; Tang, C. W. *Appl. Phys. Lett.* **1996**, *69*, 2160.

(10) Curioni, A.; Andreoni, W. *J. Am. Chem. Soc.* **1999**, *121* 8216.

(11) Curioni, A.; Boero, M.; Andreoni, W. *Chem. Phys. Lett.* **1998**, *294*, 263.

(12) Curioni, A.; Andreoni, W. Treusch, R.; Himpsel, R. F.; Himpsel, R. F.; Haskal, E.; Seidler, P.; Kakar, S.; van Buure, T.; Terminello, L. J. *Appl. Phys. Lett.* **1998**, *72*, 1575.

(13) Johansson, N.; Osada, T.; Stafstrom, S.; Salaneck, W. R.; Parente, V.; dos Santos, D. A.; Crispin, X.; Bredas, J. L. *J. Chem. Phys.* **1999**, *111* 2157.

(14) Halls, M. D.; Aroca, R. *Can. J. Chem.* **1998**, *76*, 1730.

(15) Kushto, G. P.; Lizumi, Y.; Kido, J.; Kafafi, Z. H. *J. Phys. Chem. A* **2000**, *104*, 3670.

(16) Amati, M.; Lelj, F. *Chem. Phys. Lett.* **2002**, *363*, 451.

(17) Su, Z.; Cheng, H.; Gao, H.; Sun, S.; Chu, B.; Wang, R.; Wang, Y. *Chem. J. Chin. Univ.* **2000**, *211*, 416.

(18) Anderson, S.; Weaver, M. S.; Hudson, A. J. *Synth. Met.* **2000**, *111*−*112*, 459.

(19) Martin, R. L.; Kress, J. D.; Campbell, I. H.; Smith, D.L. *Phys. Rev. B* **2000**, *61*, 15804.

(20) Stampor, W.; Kalinowski, J.; Marconi, G.; Di Marco, P.; Fattori, V.; Giro, G. *Chem. Phys. Lett.* **1998**, *283*, 373.

(21) Bacon, A. D.; Zerner, M. C. *Theor. Chim. Acta* **1979**, *53*, 21.

(22) Halls, M. D.; Schlegel, H. B. *Chem. Mater.* **2001**, *13*, 2632.

(23) Sugimoto, M.; Sakaki, S.; Sakanoue, K.; Newton, M. D. *J. Appl. Phys.* **2001**, *90*, 6092.

(24) Cölle, M.; Dinnebier, R. E.; Brütting, W. *Chem. Commun.* **2002**, 2908.

(25) Zhang, J. P.; Frenking. G. *J. Phys. Chem. A* **2004**, *108*, 10296.

(26) Kepler, R. G. *Phys Rev.* **1960**, *119*, 1226.

(27) LeBlanc, O. H. *J. Chem. Phys.* **1961**, *35*, 1275.

(28) Pope, M.; Swenberg, C. E. *Electronic Progresses in Organic Crystals;* Oxford University Press: New York, 1982.

(29) Silinsh, E. A.; Capek, V. *Organic Molecular Crystals: Interaction, Localization, and Transport Phenomena;* AIP, New York, 1994.

(30) Jurchescu, O. D.; Baas, J.; Palstra, T. T. M. *Appl. Phys. Lett.* **2004**, *84*, 3061.

(31) Karl, N.; Marktanner, J.; Stehle, R.; Warta, W. *Synth. Met.* **1991**, *42*, 2473.

(32) Torsi, L.; Dodabalapur, A.; Rothberg, L. J.; Fung, A. W. P.; Katz, H. E. *Science* **1996**, *272*, 1462.

(33) Nam, M. S.; Ardavan, A.; Cava, R. J.; Chaikin, P. M. *Appl. Phys. Lett.* **2003**, *83*, 4782.

(34) Lin, B. C.; Cheng, C. P.; You, Z. Q.; Hsu, C. P. *J. Am. Chem. Soc.* **2005**, *127*, 66.

(35) Brédas, J. L.; Beljonne D.; Coropceanu, V.; Cornil, J. *Chem. Rev.* **2004**, *104*, 4971.

(36) Lemaur, V.; da Silva Filho, D. A.; Coropceanu, V.; Lehmann, M.; Geets, Y.; Piris, J.; Debije, M. G.; van de Craats, A. M.; Senthilkumar, K.; Siebbeles, L. D. A.; Warman, J. M.; Cornil, J. *J. Am. Chem. Soc.* **2004**, *126*, 3271.

(37) Brédas, J. L.; Calbert, J. P.; da Silva Filho, D. A.; Cornil, J. *Proc. Natl. Acad. Sci. U.S.A.* **2002**, *99*, 5804.

(38) Cornil, J.; Beljonne, D.; Brédas, J. L. *Adv. Mater.* **2001**, *13*, 1053.

(39) Lehmann, M. D.; Lemaur, V.; Cornil, J.; Brádas, J. L.; Goddard, S.; Grizzi, I.; Geerts, F. *Chem. Mater.* **1995**, *7*, 1337; Cornil, J.; Lemaur, V.; Calbert, J. P.; Brádas, J. L. *Adv. Mater.* **2002**, *14*, 726.

(40) Cheng, Y. C.; Silbey, R. J.; da Silva Filho, D. A.; Calbert, J. P.; Cornil, J.; Brádas, J. L. *J. Chem. Phys.* **2003**, *118*, 3764.

(41) Hannewald, K.; Bobbert, P. A. *Appl. Phys. Lett.* **2004**, *85*, 1535; Hannewald, K.; Stojanovic, V. M.; Schellekens, J. M. T.; Bobbert, P. A.; Kresse, G.; Hafner, J. *Phys. Rev. B* **2004**, *69*, 075211.

(42) Troisi, A.; Orlandi, G. *J. Phys. Chem. B* **2005**, *109*, 1849.

(43) Schmidbaur, H.; Lettenbauer, J.; Wilkinson, D. L.; Müller, G.; Kumberger, O. Z. *Z. Naturforsch. B* **1991**, *46*, 901.

(44) Fujii, I.; Hirayama, N.; Ohtani, J.; Kodama, K. *Anal. Sci.* **1996**, *12*, 153.

(45) Brinkmann, M.; Gagret, G.; Muccni, M.; Taliani. C.; Mascinocchi, N.; Sironi, A. *J. Am. Chem. Soc.* **2000**, *122*, 5147.

(46) Cölle, M.; Gmeiner, J.; Milius, W.; Hillevrecht, H.; Brütting, W. *Adv. Funct. Mater.* **2003**, *13*, 108.

(47) Delley, B. *J. Chem. Phys.* **1990**, *92*, 508.

(48) Delley, B. *J. Chem. Phys.* **2000**, *113*, 7756.

(49) Monkhorst, H. J.; Pack, J. D. *Phys. Rev. B* **1977**, *16*, 1748.